Journal of the National Academy of Forensic Engineers®

http://www.nafe.org

ISSN: 2379-3252

DOI: 10.51501/jotnafe.v43i1

Vol. 43 No. 1 June 2026

Investigating Effects of Imperfections on Aluminum Stepladder Using Finite Element Analysis

By John Thomazin, PE, DFE (NAFE #1188M), Bill Webster, and Sai Kosaraju, PhD

Abstract

Ladders are a valuable tool, but they can also be dangerous. In 2020, ladder-related falls resulted in more than 100 fatalities and thousands of injuries, particularly in the installation, maintenance, and repair industries [1]. The ANSI A14.2 standard governs the safe construction, design, testing, and use of portable metal ladders, outlining requirements for ladder rung spacing, connections, and angle of inclination. While 15 different load tests are performed to ensure a ladder meets the standard, it's important to note that these tests use statistical tolerances and represent pass/fail criteria. Altering the cross-section of a shape can impact its stiffness, and imperfections can affect a structure's collapse. Understanding the testing limitations is crucial. To reduce ladder-related injuries and fatalities, imperfection-sensitive ladders can be detected, evaluated, and identified using 3D modeling and nonlinear finite element analysis (FEA). This paper presents a technique for using linear-elastic buckling analysis to identify potential failure modes. It is followed by nonlinear static analysis with material plasticity to detect significant decreases in strength when dents or other imperfections are included in the geometry or when the applied load directions are changed.

Keywords

Forensic engineering, finite element analysis, FEA, structural safety, ladder design, fall-related injuries, ANSI standards A14.2, load testing, workplace safety, imperfection sensitivity, 3D modeling, simulation, computer-aided engineering, CAE

Ladder Hazards & Injuries

The stepladder is a mechanical linkage consisting of front and back rails connected with spreaders that are used to lock the front and back rails in the open position. Steps on the front rails are spaced at approximately 1-foot intervals. Once the stepladder is locked in position, the feet form a base along with the four rails, creating two basic triangles that form a rigid, stable framework suitable for climbing.

Ladders, a tool in use for more than 10,000 years, have seen significant advancements in safety. The first practical folding stepladder was invented by John H. Balsley, a skilled carpenter from Pennsylvania. His patent in 1862 marked a significant improvement in ladder safety, as he replaced round rungs with flat steps and added hinges for easy folding and storage when not in use [2].

Ladders are useful tools both at home and at the worksite; however, they can also be dangerous. Many hospital visits result from ladder falls. According to the National Institute for Occupational Safety and Health (NIOSH), ladder-related falls account for more than 100 fatalities and thousands of injuries each year [1]. In 2020, there were 22,710 injuries caused by ladder-related falls, compared with 22,330 in 2019. The installation, maintenance, and repair occupations had the highest ladder-related injuries — with 5,790 incidents reported. Construction and extraction occupations accounted for 5,370 ladder injuries, and service occupations had 3,160 [3]. Despite efforts at improving safety and training, the number of fatalities and ladder-related injuries from falls does not change much from year to year.

John Thomazin, PE, DFE, 1925 Westbourne Dr., Oviedo, FL 32765, (407) 375-1435, jthomazin@outlook.com

Injury and Background

In the late summer of 2019, a homeowner was using a stepladder purchased from a home-improvement retail chain. As the stepladder was being used for household chores, the side rail components of the stepladder's A-frame buckled, resulting in instability, downfall, and collapse. The stepladder was allegedly not overloaded or subject to abuse at the time of the collapse. The homeowner landed on his backside and was injured by the collapse. Settlement terms of the case prevent disclosure of the parties' names and product brands. The subject stepladder was sold throughout the United States and distributed through major home-improvement retail chains. The subject stepladder is made of aluminum and has a rated load capacity of 250 pounds.

ANSI Standards and Certifications

The subject stepladder is marked with the American National Standards Institute (ANSI) A14.2, Occupational Safety and Health Administration (OSHA) certification label. The Metal Ladder Manufacturers Association is responsible for initiating the ANSI standard for portable metal ladders, dating back to May 1951. The ANSI 14.2 standard prescribes rules governing the safe construction, design, testing, care, and use of portable metal ladders of various types and styles [4].

As shown in **Figure 1**, there are five duty ratings and ladder types with working-load limits ranging from 200 pounds to 375 pounds. According to the label on the subject stepladder, the ladder's size was 6 feet, the maximum reach was 10 feet, and the highest standing level was 3 feet, 10 inches. It has a tray for holding tools or one paint can and slots for a roller tray. As such, the subject ladder would be considered "light duty."

Development of ANSI Ladder Standards

The prescriptive standard aims to provide reasonable safety for life, limb, and property. The voluntary standard on portable ladders is one of many American National Standards prepared under the ANSI Accredited Standards Committee on Safety in the Construction, Care, and Use of Ladders (A14). The subcommittee for portable metal ladders is A14.2.

Duty Rating	Ladder Type	Working Load (lb)	Size (ft)
Special Duty	IAA	375	3-12
Extra Heavy Duty	IA	300	3-20
Heavy Duty	I	250	3-20
Medium Duty	II	225	3-12
Light Duty	III	200	3-6

Figure 1
Classification of stepladders by duty rating, type, and size.

Section five of A14.2 outlines portable metal ladders' general safety and performance criteria. The requirements are kept to a minimum to allow for various combinations of metals and design alternatives when designing and constructing the ladders. This section specifies dimensions such as rung spacing, width, and height, ensuring the ladders provide a stable and comfortable climbing experience. Other features, such as rungs, steps, and railings, must comply with safety specifications regarding size and shape. Designers and manufacturers must ensure that ladders are designed and constructed to safely support the loads they will encounter during use, accounting for strength, durability, and stability. The construction materials must be high-quality and appropriate for ladder manufacturing. Furthermore, the design must ensure that the ladder is strong and stiff enough to meet the performance requirements of this standard and is free from structural defects or accident hazards, such as sharp edges or burrs.

The standard outlines the safe construction, design, testing, care, and use of metal ladders. The testing procedures in section seven were developed for three applications: design verification, quality control, and in-service testing. During the original design development of the product, design verification tests are generally conducted as destructive tests. The manufacturer performs quality control tests on an ongoing basis, including both destructive and nondestructive tests.

The standard's remaining sections outline the most appropriate procedures for ladder care, selection, and use. They also specify the required labeling and product data information marks for the different types of ladders.

Investigation and Examination

For the subject incident investigation, the homeowner was available for an interview, and the room where the fall happened was measured, photographed, and 3D-scanned. The subject stepladder was also measured and photographed. The assembled stepladder framework uses rivets to fasten aluminum and plastic components into the finished product. The braced aluminum side rails are open-section C-shaped members joined by steps, rungs, cleats, or rear braces at regular intervals. The thickness of the aluminum side rails connecting the rungs was approximately 14 gauge (0.0747

inches). The aluminum back rails are open-section C-shaped members with unequal legs. The thickness of the aluminum back rails was approximately 13 gauge (0.0897 inches). The diameter of the rivets was approximately $^{3}/_{16}$ inches. The subject stepladder generally met the requirements of Section 5 and the specifications of section 6 of ANSI A14.2. Additionally, it fulfilled the labeling/marking requirements of Section 9.0 in ANSI 14.2.

According to A14.2 requirements, the physical loads on the stepladder, and the homeowners' description of use before the collapse, the ladder should not have collapsed. The stepladder was set up on carpet, and the floor was even and firm. The homeowner weighed approximately 160 pounds — well below the ladder's working load limit. According to the claimant, at the time of the incident, the stepladder was not overloaded, and the weight was centered on its base. As shown in **Figure 2**, the right front side rail of the stepladder buckled near the first rung and braces by the connections. Overall, buckling initiated below the lower rung near the connections along the shorter, horizontal axis of the two front-side rails.

Exemplar Ladder

An exemplar ladder was purchased for comparison. The exemplar and subject ladders were manufactured at the same plant four years apart. The authors photographed, measured, and documented the exemplary ladder and used those measurements to create a 3D CAD model, which could then be used in FEA simulation software.

Manufacturer's Testing

The test requirements in A14.2 Section seven are preferred methods to determine whether a ladder conforms to the standard's requirements. The tests that were developed for the standard use statistical methods. If a single test fails, then the test can be repeated using a sufficient sample size to ultimately determine whether a ladder passes or fails a test. In the case of a stepladder, various loads are placed on it — usually for 1 minute. If the ladder does not collapse or permanently deform after the test, it has passed. In all, there are about 15 different load tests for a stepladder. This analysis addresses only one test: the *Torsional Stability Test*, which is a design verification test.

After the incident, the manufacturer performed physical testing on the exemplar stepladder to recreate the damage and deformation seen in the subject stepladder. The physical testing was video recorded and narrated. The testing consisted of a demonstration and modified A14.2 test cases. In the demonstration, the product tester stepped on the bottom rung of the ladder, gently lifted the front rails of the ladder, and twisted the stepladder at the top to simulate a walking motion. The implied purpose of the demonstration was to show that the stepladder could be misused without collapsing.

FEA vs. Physical Testing

The manufacturer's tests did not replicate the buckling response seen in the subject stepladder. The post-buckling damage observed in the stepladder's side rails implies a torsional loading condition or walking motion before collapse. Desired confidence intervals and error levels establish the necessary sample size for testing [5] [6]. High confidence intervals and low error levels require more test trials, and vice versa (**Figure 3**). The great advantage of computer simulation is that multiple trials can be run at a fraction of the time and labor of a physical test. In addition, the model can predict failure modes before failure. A stepladder response can forewarn of potential failure modes present in the stepladder's structure.

The torsional loading test case in ANSI 14.2 Section 7.5.12 *Rail Torsion and Spreader Test* was chosen for FEA, as shown in **Figure 4**. After the FEA analysis, ANSI physical tests could be performed, and the results compared, if needed. In Section 7.5.12, the test unit should be placed on a level floor, with a 200-pound load applied to the ladder top cap and a horizontal force applied to the top cap. The ladder should withstand the forces without damage. Ladders with a bucket shelf should be tested with

Figure 2
Buckled condition of the front side rails for the subject stepladder.

Confidence level

Error	99	95	90	85	80	75	70
0.05	664	385	271	208	165	133	108
0.1	166	97	68	52	42	34	27
0.15	74	43	31	24	19	15	12
0.2	42	25	17	13	11	9	7

Sample size needed to meet confidence interval at error level.

Figure 3
Sample size needed for various confidence intervals and error levels.

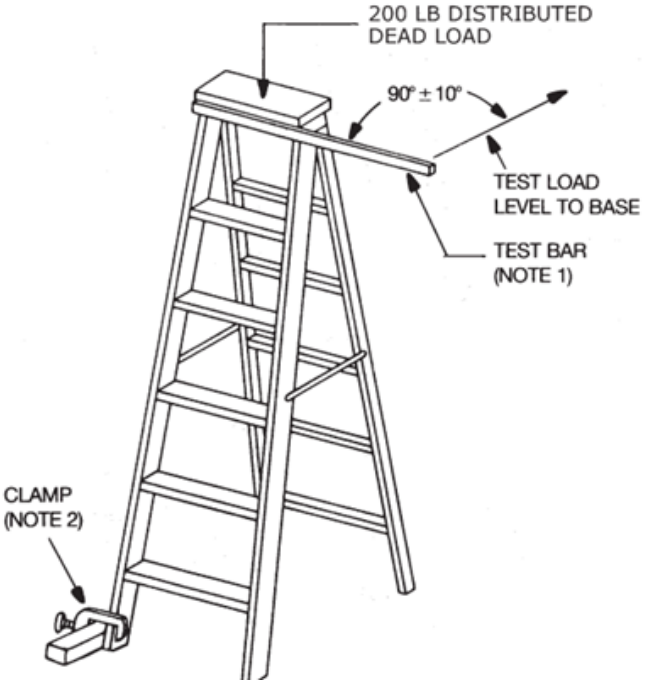

(1) The test bar is clamped to the top cap.
(2) Clamp only used for the rail torsion and spreader tests in 7.5.12.

Figure 4
Setup for rail torsion and spreader test.

the shelf in the in-use position, and step stools are exempt from this test.

The stiffness of a ladder or any framework combines material elasticity, given as Young's modulus, and geometry. The shape of individual components, combined with the overall assembled geometry of the structure, determines the framework's stiffness. Changing the cross-section of a shape can increase or decrease its stiffness. Dimensionally larger cross-sections are generally stiffer than dimensionally smaller cross-sections. To change the stiffness and affect a favorable response, a designer can change either material, geometry, or a combination of both geometry and material. Gaining insight into the response of the stepladder's assembled framework to external loads can start with an understanding of the response of individual components to external loads.

The buckling of bars, frames, plates, shells, or other members is a response to compressive axial loads. Buckling occurs when a member converts membrane strain energy into bending strain energy without changing externally applied loads [7, Ch. 14]. There is no forewarning when conditions become critical — that moment when buckling is imminent — and any slight change in the deformation state triggers an instant conversion of membrane energy to bending energy. Comparatively, a member can store huge amounts of membrane strain energy, but bending strain energy can only absorb the released membrane energy with large lateral deflections and cross-sectional rotations. In other words, buckling occurs without forewarning when compressive forces reduce the bending stiffness to near-zero for some deformation mode, and potential energy rapidly converts to kinetic energy with large lateral deformations.

FEA is a good tool for gaining insight into stress distribution throughout ladder components before the onset of buckling behavior. Both a limit-state analysis and a computer-aided linear-bifurcation buckling analysis may over-predict the failure load of a structure. The goal of the forensic engineer is to understand if the structure loses strength when applied to various loads.

The post-buckling response of a structure becomes nonlinear, and stiffness is reduced. A loss of stiffness can result in large deformations without any increase in load. In that case, the performance of a structure is strongly affected by small changes in the direction of the loads, the manner of support, or changes in the structure's geometry. Changing the geometry of the structure or cross-sectional properties of a member is an effective means for favorably changing the response of a structure to prevent collapse. Accordingly, FEA is an effective technique for modeling the effects of changes.

Finite Element Model and Workflow

The initial step in any simulation process, following thorough research and planning, is generating an appropriate model for analysis. Broadly, this entails creating a finite element mesh, applying relevant material and section properties, modeling connections, interactions, or contact phenomena, and finally, constraining and loading the structure. While the process may appear straightforward, it requires significant expertise and a deep understanding of physics to be executed correctly. The FEA workflow for evaluating buckling sensitivity generally unfolds in four stages, as depicted in **Figure 5**.

Following the creation of a detailed ladder model, a linear buckling analysis was performed to estimate buckling loads, yielding results comparable to those from hand calculations. Although this analysis is relatively simple and based on linear assumptions, it offers several advantages. First, it provides a more efficient method for conducting traditional buckling calculations on complex

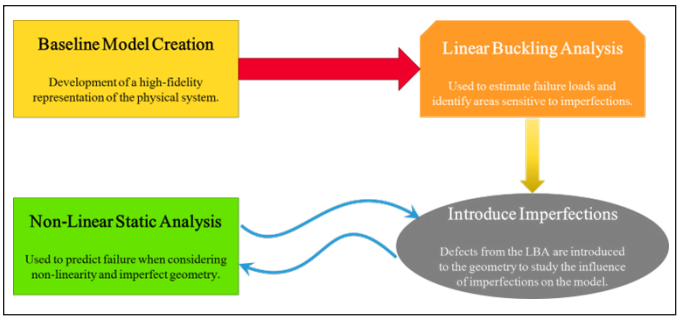

Figure 5
General workflow for FEA buckling model creation and analysis.

structures compared to manual calculations using free-body diagrams and spreadsheets. More importantly, it identifies potential failure locations in the structure and predicts the failure mode or shape. This information empowers engineers to make qualitative design improvements, alter load paths, and adjust boundary conditions to mitigate risks of failure. Additionally, linear buckling analyses are computationally inexpensive, allowing for the rapid evaluation of design alternatives. For reference, each buckling simulation was completed in approximately 3 minutes.

In the subsequent workflow phase, geometric imperfections were introduced to assess sensitivity to various defects. The authors examined thickness and section defects by reducing the thickness of the front leg and shortening the length of the C-channel flange. Shape defects were also explored, although their introduction posed challenges in terms of model implementation. Determining the defect's size, shape, and placement within the model required careful consideration to ensure a meaningful impact on the results. By leveraging the buckled shapes from the linear buckling analysis, the authors ensured that imperfections were properly sized, shaped, and positioned to yield worst-case scenarios.

The final phase involved conducting a nonlinear static analysis on both the baseline geometry and the models with geometric defects. This analysis considers material plasticity, load redistribution, section changes, contact, and stress stiffening, making it more realistic than linear analyses or hand calculations.

Material and Model Discretization

Creating a model for FEA begins with a thorough understanding of the material properties. In the absence of specific material properties for the ladder under investigation, the authors used properties for 6061-T6 aluminum, which are well-documented in existing literature. Aluminum 6061-T6 is recognized for its favorable mechanical properties, corrosion resistance, widespread availability, and relatively low cost compared to other aluminum alloys. They referenced MMPDS-04 [8], a key standard for metal material properties in the aerospace industry (**Figure 6a**), to obtain engineering properties such as Young's modulus, yield strength, ultimate strength, and elongation — necessary for defining the model's material behavior (**Figure 6b**).

The nonlinear stress-strain behavior was approximated using the Ramberg-Osgood equation, which has shown excellent correlation with physical test data for metals such as steel, aluminum, and titanium. This method, developed in 1943, relates strain to stress, Young's modulus, a material-specific strength coefficient, and a material-specific hardening coefficient. These coefficients can be calculated using readily available engineering data, making it a convenient method for approximating nonlinear material behavior without the need for test data.

The ladder model included aluminum components as well as plastic and rubber parts. The top cap was made from ABS plastic, and the ladder feet were made of rubber. Linear elastic material properties were used for the ladder cap, as it was not a primary focus and was not subjected to significant stress. The rubber feet were omitted from the model due to their minimal structural impact.

The modeling approach employed shell elements for the main structural components, a process known as

FEA Material Properties						
Component	Material	Young's Modulus (ksi)	Poisson's Ratio	Yield Strength (ksi)	Ultimate Strength (ksi)	Elongation (%)
Structural Components	6061-T6 Aluminum	9900	0.33	35	42	16
Plastic Cap	ABS Plastic	350	0.37			

Figure 6a
Aluminum 6061 material properties.

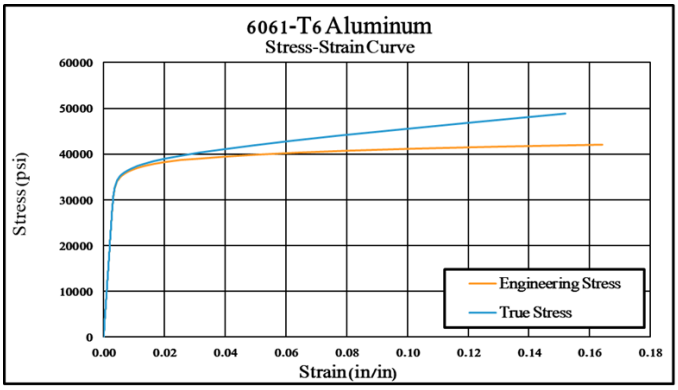

Figure 6b
Aluminum 6061 material behavior modeled by FEA.

midplaning, which involves creating a 2D mesh to represent a 3D structure. While this approach might initially seem counterintuitive, shells provide the most accurate and cost-effective solution for modeling thin-walled structures under bending. A 1-inch mesh size was primarily used, which, although relatively large, was sufficient to generate an accurate stiffness matrix and predict correct displacements. However, the large mesh size may result in non-converged stress values, which were addressed by locally refining the mesh near failure locations. Sensitivity studies determined the appropriate mesh size in these areas, ultimately settling on a 3-millimeter mesh size in regions near the bottom of the front left leg and the proximal angle braces, as shown in **Figure 7**.

The connection of the ladder structure was simplified using TIED constraints (an Abaqus keyword) to bond neighboring components at the overlapping interface, rather than modeling the complexity of rivets and associated contact between components. This level of detail was deemed sufficient because the failure mode was not related to the joints, and the load path could still be accurately captured using TIED constraints. This approach is also supported by St. Venant's principle, which posits that the exact distribution of load near the point of application does not significantly affect the stress distribution at a distance, thereby ensuring global accuracy despite local modeling simplifications.

Boundary Conditions and Loads

With a highly accurate simulation model created, the next step was to constrain and load the model to replicate the test conditions outlined in ANSI A14.2. The front left leg of the ladder was fully clamped to prevent all translation and rotation, while the other three legs were c onstrained only in the downward direction, allowing them to slide or lift off the ground — similar to a ladder on a frictionless surface.

The ladder was loaded according to ANSI A14.2, with a 200-pound distributed dead load applied downward on the ladder's top cap. A rigid bar was clamped to the top cap, and a rearward load was applied to that rigid bar 18 inches from the ladder's longitudinal centerline (**Figure 8**).

FEA Analysis Techniques

Finite element analysis was conducted using Abaqus 2024 [9] to examine the structural response of a ladder under loads similar to those outlined in ANSI A14.2. As summarized in **Figure 9**, the study involved two types of analyses: linear buckling analysis and nonlinear static analysis. Linear buckling analysis is akin to arithmetic, providing

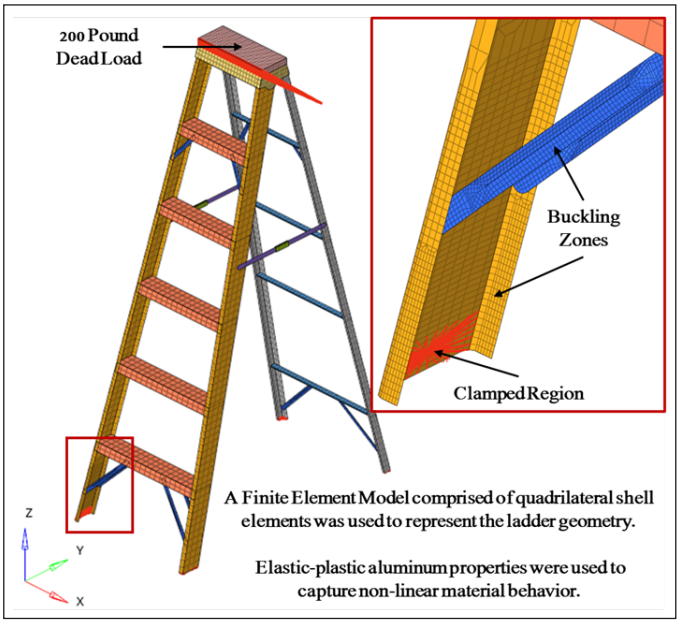

Figure 7
Finite element model of the stepladder.

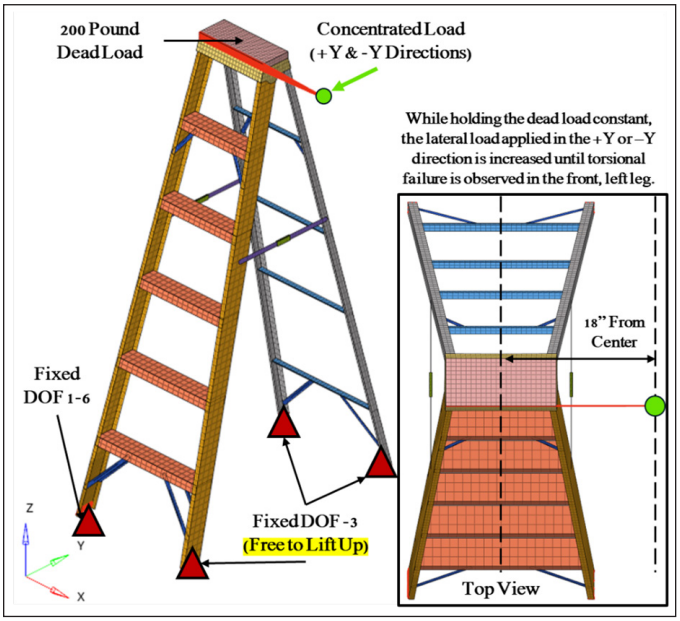

Figure 8
Loading and boundary conditions of the stepladder.

Linear Buckling Analysis	Nonlinear Static Analysis
• Used to estimate the critical bifurcation load of stiff structures.	• Used to evaluate the non-linear structural response to loading.
• Inherently linear: elastic material properties & linear geometry only.	• Considers material plasticity and changes to geometry arising from loading-induced deformation.
• Can be used to extract deformed shapes used in subsequent imperfection sensitivity analyses.	• Used to understand the non-linear force-deflection behavior of a system.
• Useful in identifying collapse mode shapes but can often overestimate failure loads due to inherent linearity.	• Provides a more accurate solution by accounting for non-linearities that may arise prior to elastic buckling.

Figure 9
Summary of analysis techniques used in the FEA study.

a simple and efficient method for estimating critical bifurcation loads in stiff structures. Nonlinear static analysis (comparable to calculus) accounts for material plasticity, load redistribution, and geometric changes, yielding more accurate results for complex scenarios.

Linear buckling analysis predicts elastic buckling by estimating the critical bifurcation load, offering accurate and cost-effective quantitative results for structures experiencing true elastic buckling. However, its inherent linearity limits its accuracy, which fails to account for material plasticity, changes in loading direction, loss of section properties due to deformation, or contact between neighboring bodies. As a result, linear buckling analyses often overestimate the magnitude of buckling failure, particularly in structures that experience significant material yielding.

In contrast, nonlinear static analysis evaluates a system's nonlinear structural response, accounting for material, geometric, and contact nonlinearities. This method provides a deeper understanding of the true physics involved and yields more accurate results than linear analyses.

Linear Buckling Analysis Results

The linear buckling analysis results shown in **Figure 10** revealed several interesting trends. The first buckling mode occurs in the angle brace, a thin, relatively flat piece of metal loaded in compression. However, the buckling of the angle brace does not necessarily lead to the collapse of the ladder, as the front leg is the primary load-carrying member. To assess the potential for ladder collapse, it is crucial to identify the buckling mode affecting the area of interest.

When the ladder is loaded according to ANSI A14.2, the first buckling mode affecting the left front leg occurs at a load of 164 pounds, and Positive Y was applied. Interestingly, when Negative Y was applied, the first buckling mode occurs at a load of only 77 pounds — a decrease of over 50 percent compared to the baseline (**Figure 10**). This discrepancy arises due to the different stiffnesses of the C-channel under positive and negative bending moments. However, despite this discrepancy, the ladder still meets the 30-pound requirement even when loaded in the opposite direction to that which is specified by ANSI A14.2.

Linear Buckling Results				
Buckling Mode	Positive Y (ANSI Standard)		Negative Y (Opposite Direction)	
	Torsional Load (lb)	Buckling Location	Torsional Load (lb)	Buckling Location
1	31.1	Rear Brace	19.8	Forward Brace
2	67.5	Rear Brace	43.9	Forward Brace
3	114.4	Rear Brace	77.4	Leg Below Rear Brace
4	134.6	Rear Brace	80.6	Forward Brace
5	152.4	Rear Brace	81.0	Forward Brace
6	161.3	Rear Brace	83.7	Leg Below Rear Brace
7	163.9	Leg Side Wall	104.7	Forward Brace

Figure 10
Linear buckling modes with red text identifying modes likely to result in ladder collapse.

When loaded in the ANSI A14.2-specified direction, the buckling results can be animated to demonstrate that the first six modes affect the angle braces. Although the angle brace may buckle before the leg, it does not necessarily cause a collapse. However, the buckling of the side wall of the front leg, as shown in **Figure 11**, aligns with the observed failure in the field. With symmetry in the structure, modeling failure on the left front leg would be mirrored on the right front leg, which was the incident failure.

When the load is applied in the opposite direction, the buckling modes follow a similar trend, with the first several modes primarily affecting the angle braces. The third buckling mode, however, occurs at the same location where plastic failure was observed in the subject ladder, as shown in **Figure 12**.

In gathering data for analysis, the author evaluated three types of imperfections. A thickness imperfection was

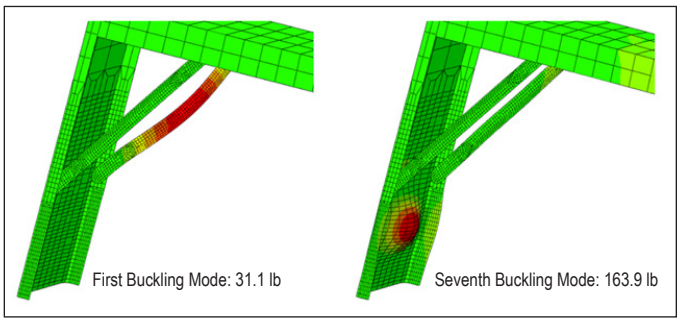

Figure 11
Linear buckling results when loaded in the +Y direction (loaded in accordance with ANSI A14.2).

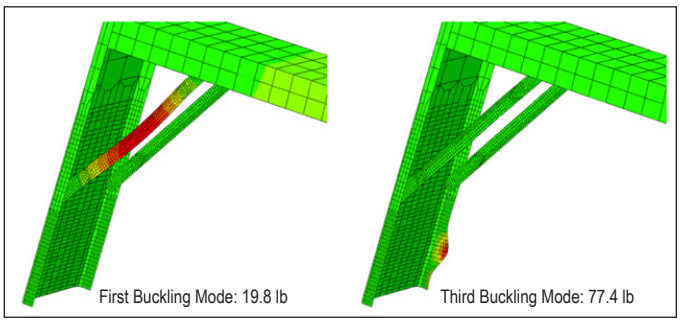

Figure 12
Linear buckling results when loaded in the Y direction (loaded in opposite direction to ANSI A14.2).

simulated by reducing the thickness of the front leg by 0.004 inches — the tolerance for 14-gauge aluminum. Section imperfections were simulated by reducing the widths of each leg flanges — first by ⅛ inches and secondly by ¼ inches. Five shape imperfections extracted from the linear buckling analysis (LBA) were introduced into the modeled geometry, as shown in **Figure 13**.

One of the key applications of LBA is the visualization of deformed shapes on the original geometry. In this research, five shape defects were examined (**Figure 13**). The selected buckling mode shapes were chosen because the modeled failures all occur within the failure zone.

Nonlinear Static Analysis Results

The nonlinear results for the baseline ladder design indicated that the ladder buckles at 62 pounds under ANSI A14.2 loading conditions. However, when loaded in the opposite direction, the failure load is reduced to approximately 23 pounds — about one-third of the forward-loading capacity. As shown in **Figure 14**, while the ladder technically meets the 30-pound ANSI requirement when loaded according to the specification, it falls short when loaded in the opposite direction, highlighting a potential code enhancement concerning buckling collapse.

Further analysis revealed the reason behind the significant difference in results. When loaded according to the ANSI standard, Von Mises stresses showed material yielding initiates on the rear flange and ultimately extends across the side wall of the front leg prior to collapse. In contrast, when loaded in the opposite direction, yielding not only initiates on the rear flange but also collapses in this region (without propagating across the side wall of the front leg).

The Maximum Principal Stress plots provide additional insight into the observed failure mechanisms. Under ANSI A14.2 torsional loading (+Y direction), tensile stresses develop in the rear flange of the front leg, suppressing local flange buckling and allowing continued load transfer. As plastic deformation progresses, stresses redistribute through the side wall of the front leg, ultimately leading to global collapse driven by gross material plasticity. Conversely, when the load is applied in the opposite direction (−Y), the rear flange is placed in compression, promoting flange buckling and precipitating failure prior to significant load redistribution.

The observed behavior is further clarified by examining the ladder's force–deflection response under opposite torsional loading directions. A force–deflection curve provides a concise means of visualizing the global nonlinear response of the stepladder, including initial yielding, post-

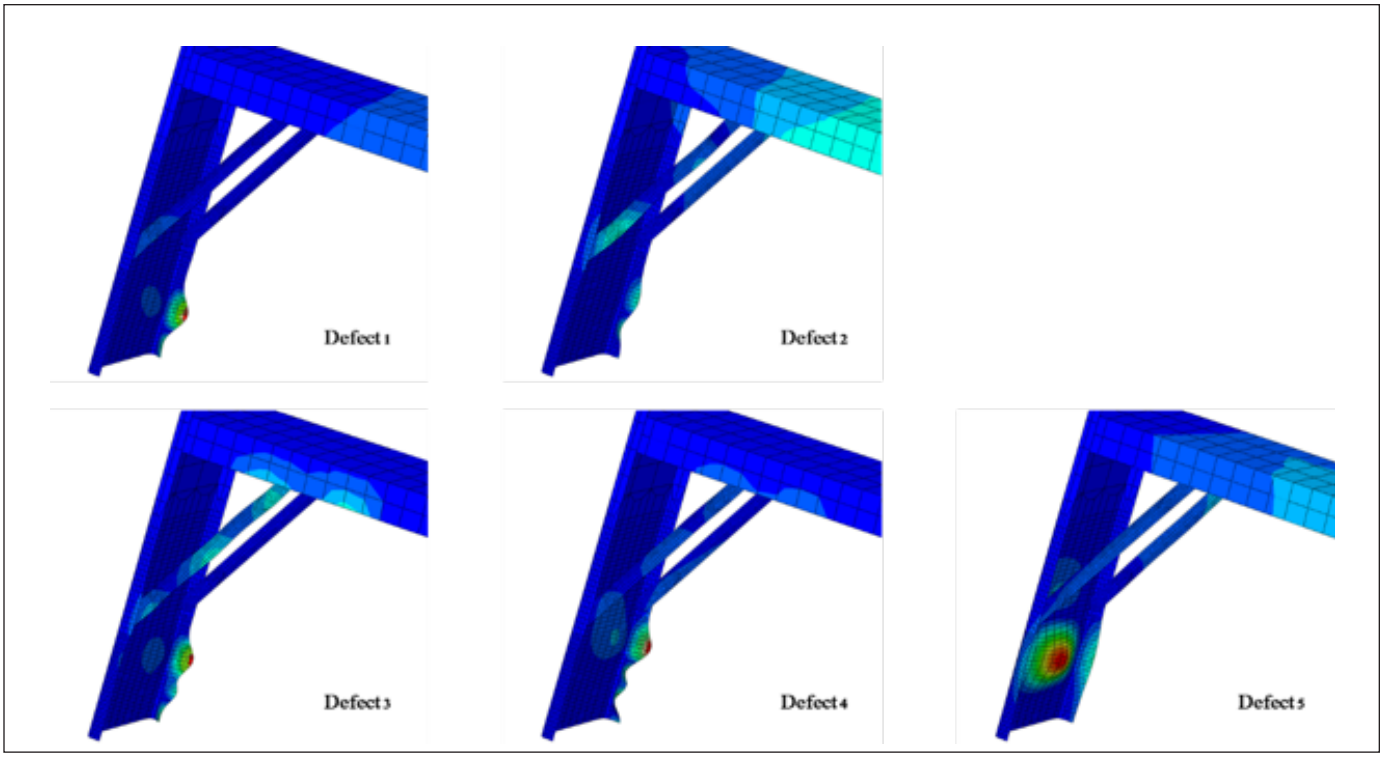

Figure 13
Imperfection definitions.

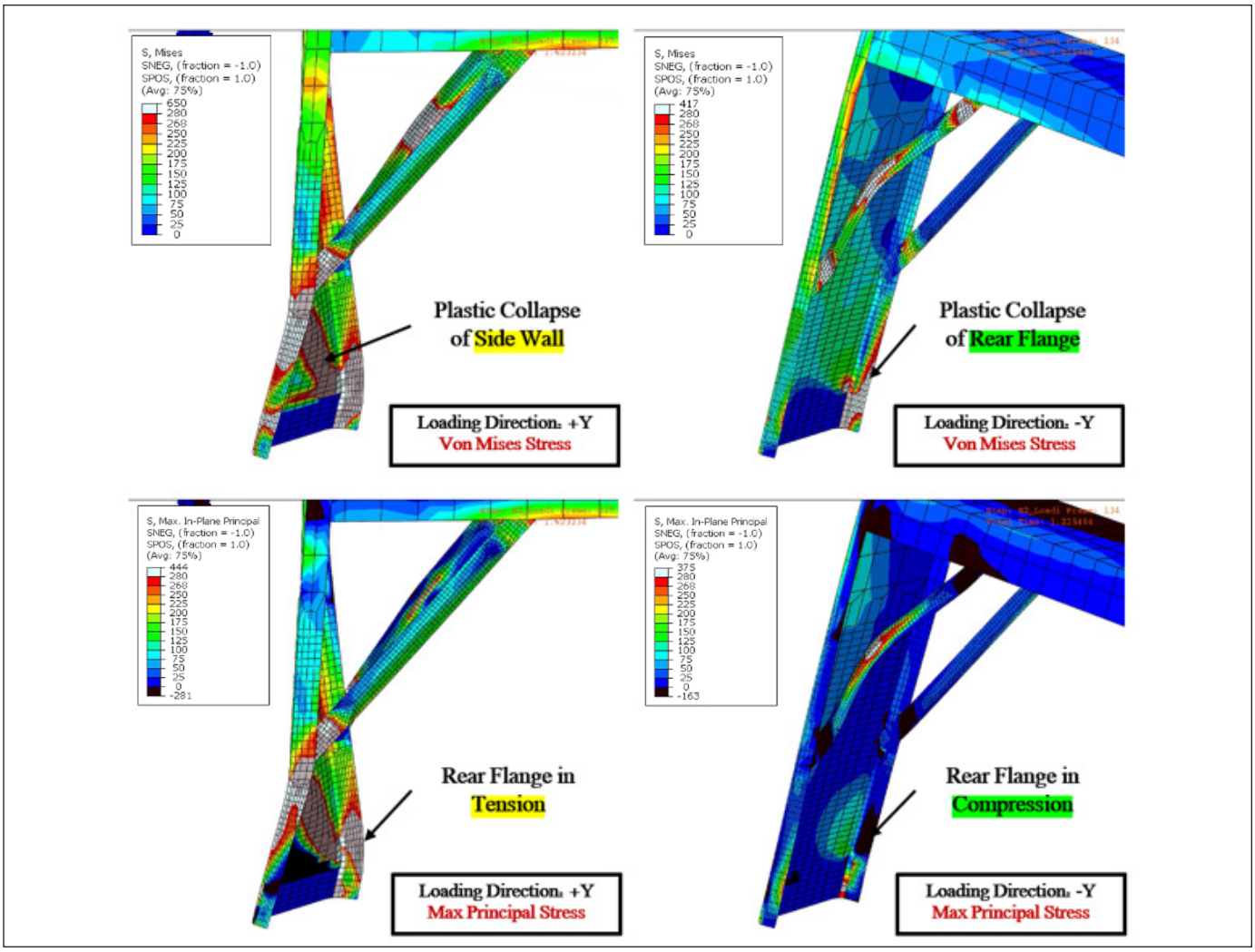

Figure 14
Nonlinear static analysis results for load directions +Y (left) and -Y (right).

buckling behavior, load redistribution, and ultimate failure.

In this study, displacement is defined as the resultant translational displacement in the global x–y plane of the node at which the torsional load is applied; specifically, the node located at the top of the stepladder on the rigid loading bar, positioned 18 inches from the ladder's centerline in accordance with ANSI A14.2. This displacement represents the motion of the rigid load application point relative to the fixed base supports and reflects the cumulative deformation of the stepladder system rather than the local deformation of an individual member. Force is defined as the applied load transmitted through the rigid loading bar at this same node in the corresponding loading direction. Both displacement and applied force were extracted directly from Abaqus as history output at the load application point and subsequently plotted to generate force-deflection curves.

When the ladder is loaded in the direction opposite the ANSI A14.2 specification (−Y direction), the force–deflection curves for the baseline and imperfect models exhibit a similar response: Initial yielding in the rear flange of the front leg is followed by a rapid loss of load-carrying capacity (**Figure 15**, left). This behavior is characteristic of flange buckling and snap-through instability, in which compressive stresses dominate and prevent significant post-yield load redistribution.

In contrast, when loaded in accordance with ANSI A14.2 (+Y direction), the force–deflection response shows a distinctly different progression (**Figure 15**, right). Tensile yielding initiates in the rear flange of the front leg, suppressing flange buckling and allowing the structure to continue carrying load. As plastic deformation develops, load redistributes into the side wall of the front leg, producing a transient stiffening response before the onset of

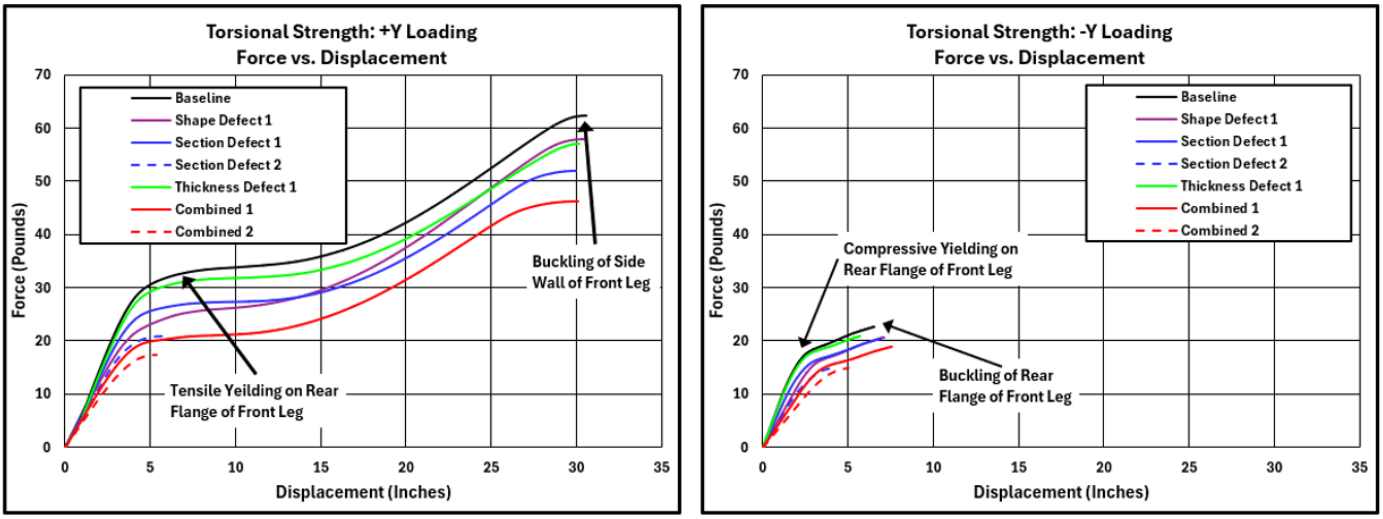

Figure 15

Force-deflection response from nonlinear static analyses for torsional loading applied in accordance with ANSI A14.2, where displacement denotes the resultant in-plane (x–y) translation of the load application node at the top of the stepladder (located 18 inches from the centerline on the rigid torsional loading bar), and force denotes the corresponding applied load transmitted through the rigid loading bar.

global collapse due to gross material plasticity. The larger displacement values observed in these curves reflect continued global deformation of the ladder assembly under sustained load redistribution, rather than excessive deformation of an individual member. For clarity and comparison, all force–deflection plots were generated using consistent axis scales. While this approach introduces unused plot space in some cases, it enables direct visual comparison between loading directions and imperfection cases without rescaling effects.

The Sensitivity of the Structure to Imperfections

The analysis of the ladder's sensitivity to imperfections revealed that nearly all introduced defects negatively impacted performance. As tabulated in **Figure 16**, the combination of multiple defects had a particularly significant impact, with strength reductions ranging from 16 to 72 percent, depending on the severity of the section change and loading direction.

Reducing section properties had the most pronounced impact on strength among the individual contributors. However, the presence of shape defects or dents in the geometry had a similar effect on performance, as did thickness reductions, despite the relatively small size of the introduced dents.

Conclusion

Physical testing is inherently constrained by time, labor, and the limited number of samples. However, FEA offers a robust alternative, demonstrating that variations in load and geometry can significantly reduce the stepladder's stiffness. When utilized correctly, FEA becomes a powerful tool for forensic investigation, enabling far more sophisticated calculations than traditional hand methods. It enables rapid iteration across designs and provides critical insights into weakening behavior that would be difficult (if not impossible) to predict with conventional approaches. Additionally, FEA software can generate compelling animations that often communicate complex information more effectively than technical data presented in spreadsheets.

The key findings of this study include the following:

1. **Loading Direction Sensitivity**: Both elastic and nonlinear analyses revealed a significant variation in performance, depending on the loading direction. Buckling response was more severe when loading was applied in the direction opposite that specified by ANSI A14.2, suggesting that the current ANSI A14.2 specification may not fully predict the buckling behavior of stepladders.

2. **Limitations of Linear Buckling Analysis**: While linear buckling analysis is effective for identifying potential failure points within a structure, it may overestimate the buckling load due to its inability to account for material plasticity, contact, or section changes.

3. **Localized Buckling vs. Structural Collapse**: The presence of localized buckling does not always signal an imminent structural collapse. Individual components can often buckle without compromising the overall stability of the structure, as seen with angle braces versus the front leg.

4. **Impact of Nonlinearities**: The nonlinear static analysis results indicated a significant decrease in performance when nonlinearities, particularly plasticity, were considered, compared to traditional elastic approaches. This underscores the importance of understanding the system's true physical behavior. An inexperienced analyst might overlook these nonlinearities when assessing buckling, potentially leading to under-design for a given load case. In contrast, experienced engineers can interpret these complexities and adapt their approach accordingly.

5. **Effect of Imperfections**: The study demonstrated that imperfections can have a material impact on structural performance.

Non-Linear Static Analysis Results

Imperfection Type	Design Condition	Torsional Load (lb)			
		Positive Y (ANSI Standard)	% Change	Negative Y (Opposite Direction)	% Change
None	Baseline	62.3		22.5	
Thickness Imperfection	Reduced Gauge (0.004")	57.1	-8.3%	20.7	-8.0%
Section Imperfection	Reduced Section 1 (1/8")	52.0	-16.5%	20.4	-9.3%
	Reduced Section 2 (1/4")	20.8	-66.6%	14.9	-33.8%
Shape Imperfection	Defect 1	57.8	-7.2%	20.7	-8.0%
	Defect 2	59.8	-4.0%	20.8	-7.6%
	Defect 3	58.4	-6.3%	21.2	-5.8%
	Defect 4	57.3	-8.0%	21.9	-2.7%
	Defect 5	66.1	6.1%	22.4	-0.4%
Combined Imperfections	Combination 1 Reduced Gauge + Reduced Section 1 + Defect 1	46.1	-26.0%	18.9	-16.0%
	Combination 2 Reduced Gauge + Reduced Section 2 + Defect 1	17.3	-72.2%	13.8	-38.7%

Figure 16
Tabular summary of nonlinear static analysis results.

Acknowledgments

The authors would like to thank Joe Dexter, PE of Reliability Engineering, LLC, for contributing to this project. He played an important role in creating the 3D CAD model used to discretize the FEA model.

References

[1] "NEWSROOM FEATURE: Ladder Safety NIOSH," 2024. [Online]. Available: http://www.cdc.gov/niosh/newsroom/feature/ladder-safety.html. Accessed: Aug. 23, 2024.

[2] J. H. Balsley, "Improved Step-Ladder," U.S. Patent 34,100A, Jan. 7, 1862.

[3] "Fatal injuries from ladders down in 2020; nonfatal ladder injuries were essentially unchanged," *The Economics Daily*, Bureau of Labor Statistics, U.S. Department of Labor, 2022. [Online]. Available: https://www.bls.gov/opub/ted/2022/fatal-injuries-from-ladders-down-in-2020-nonfatal-ladder-injuries-were-essentially-unchanged.htm. Accessed: Mar. 20, 2024.

[4] ANSI-ASC A14.2 *Ladders — Portable Metal — Safety Requirements*. Chicago, IL, USA: American Ladder Institute, 2007.

[5] W. Hammer, *Product Safety Management and Engineering*, 2nd ed. Park Ridge, IL, USA: American Society of Safety Engineers, 1993.

[6] R. E. Walpole and R. H. Myers, *Probability and Statistics for Engineers and Scientists*, 4th ed. New York, NY, USA: Macmillan, 1989.

[7] R. D. Cook, D. S. Malkus, and M. E. Plesha, *Concepts and Applications of Finite Element Analysis*, 3rd ed. New York, NY, USA: John Wiley & Sons, 1989.

[8] *Metallic Materials Properties Development and Standardization (MMPDS-04)*. Columbus, OH, USA: Federal Aviation Administration and Battelle Memorial Institute, 2008. [Online]. Available: http://app.knovel.com/hotlink/toc/id:kpMMPDSM01/metallic-materials-properties.